Supporting Information

Ultrathin 2D/2D $ZnIn_2S_4/La_2Ti_2O_7$ nanosheets with Z-scheme heterojunction for enhanced photocatalytic hydrogen evolution

Hanbing Wang[&], Yunqi Ning [&], Qi Tang, Xueyang Li, Mengdi Hao, Qun Wei, Tingting Zhao, Daqi Lv, Hongwei Tian[*]

Key Laboratory of Automobile Materials of MOE and School of Materials Science and Engineering, Jilin University, Changchun, 130012, China

[*]Corresponding author. E-mail addresses: tianhw@jlu.edu.cn (H. Tian).

[&]These authors contributed equally to this work.

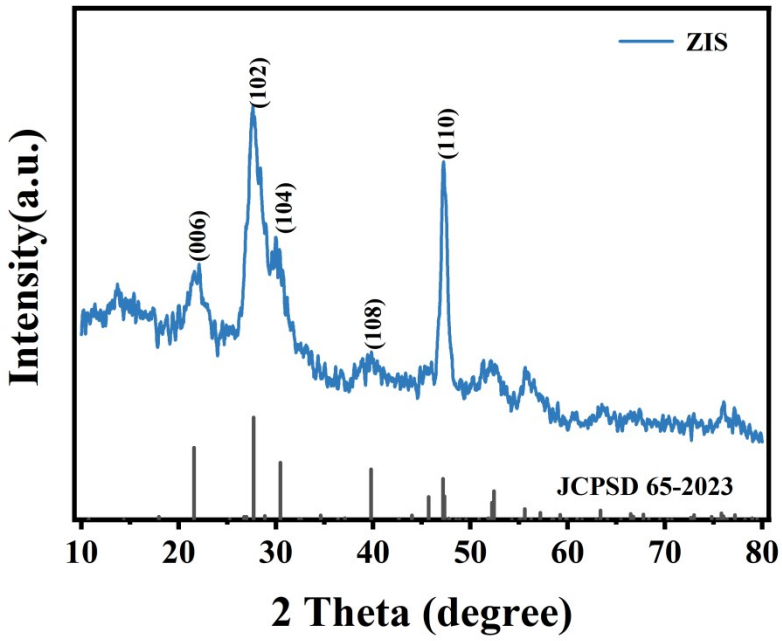

Figure S1. XRD pattern of $ZnIn_2S_4$.

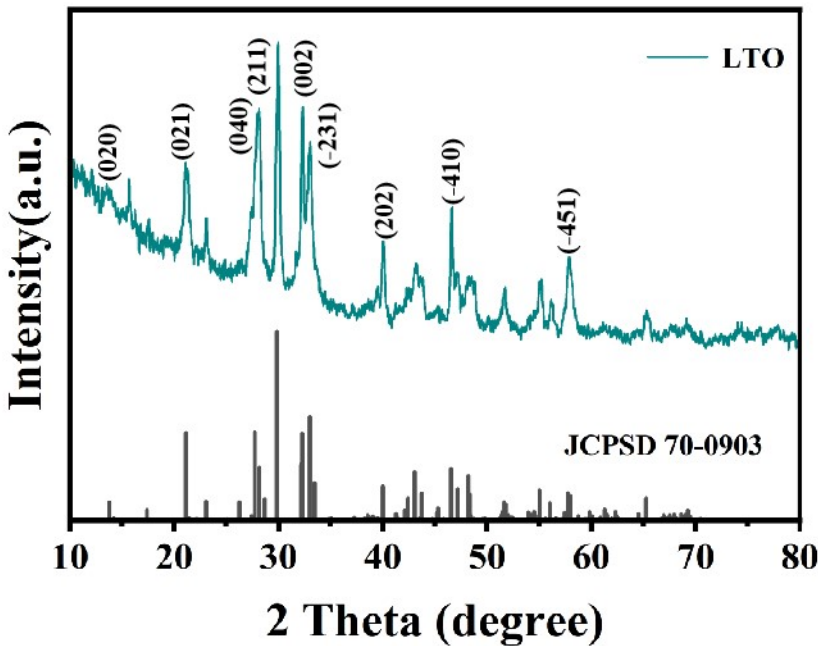

Figure S2. XRD pattern of $La_2Ti_2O_7$.

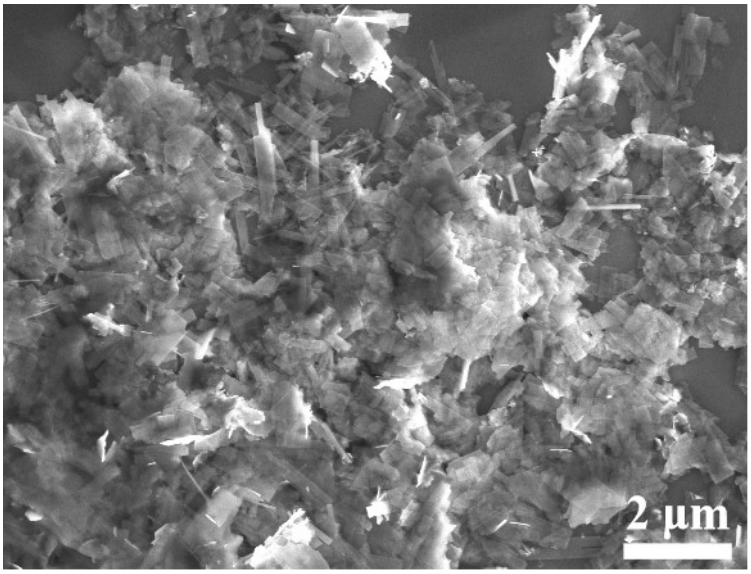

Figure S3. SEM image of $La_2Ti_2O_7$.

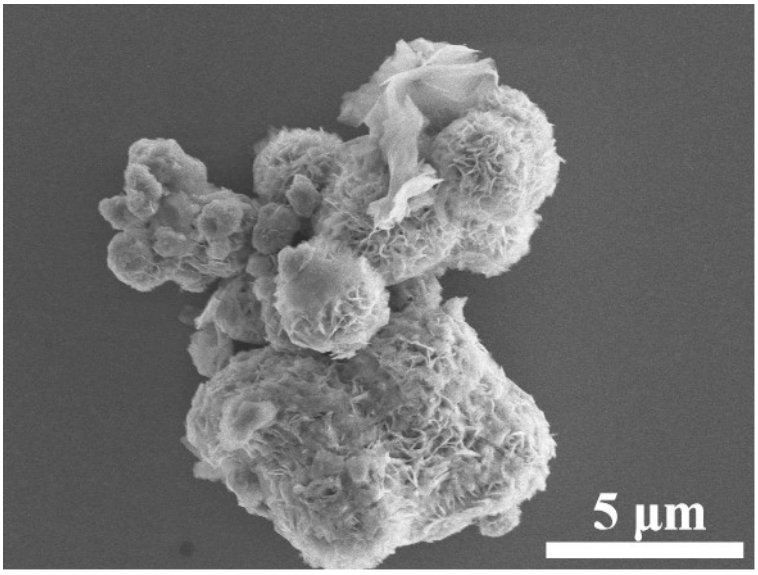

Figure S4. SEM image of $ZnIn_2S_4$.

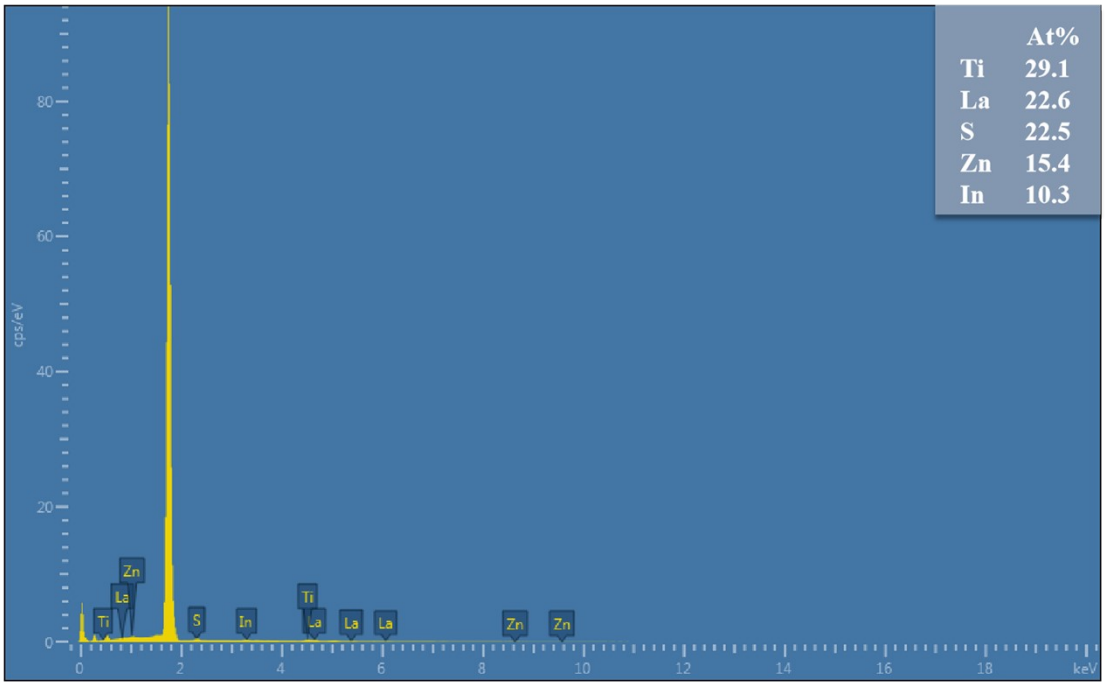

Figure S5. EDX spectrum of ZIS/LTO-0.1.

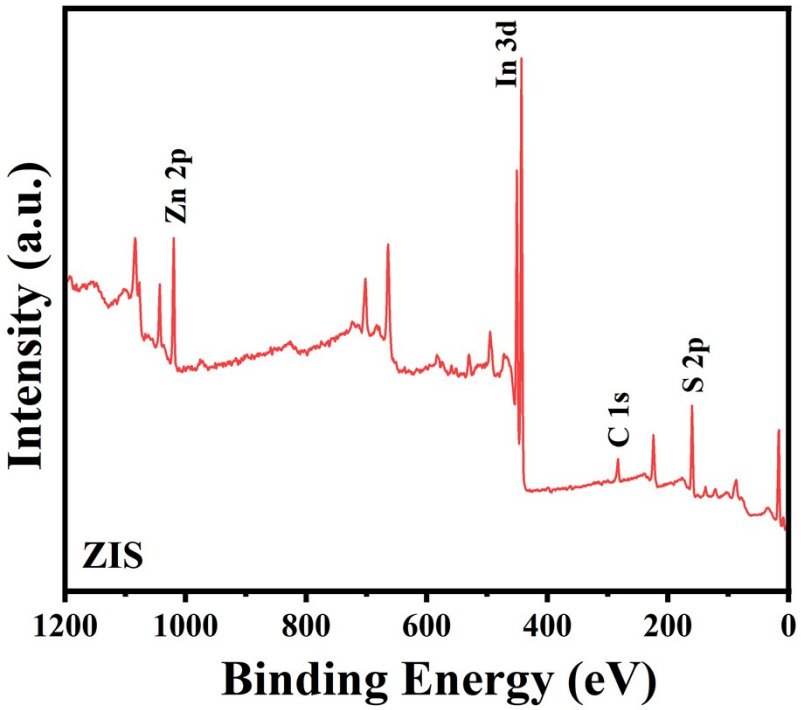

Figure S6. XPS spectra of ZIS.

.

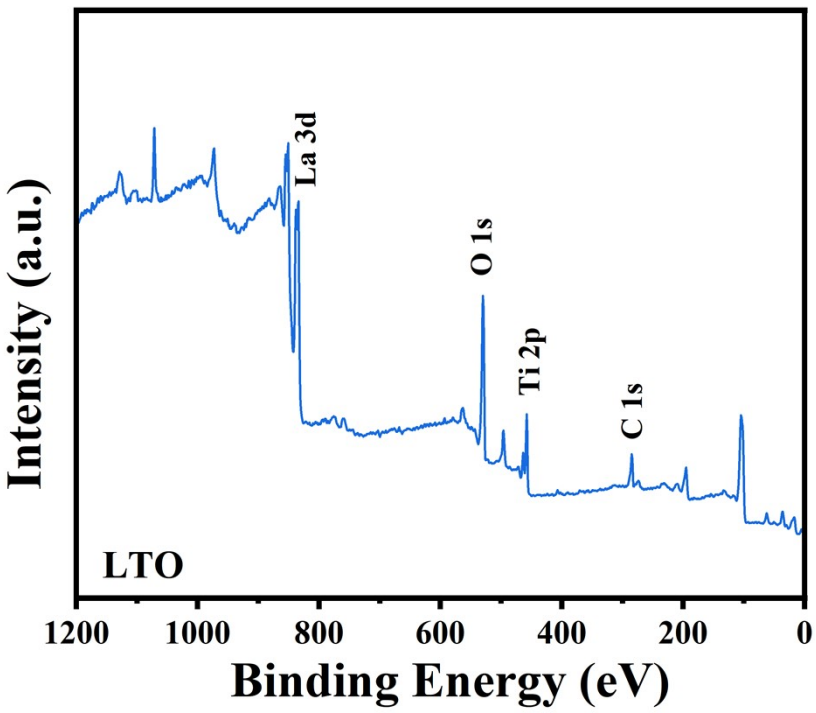

Figure S7. XPS spectra of LTO.

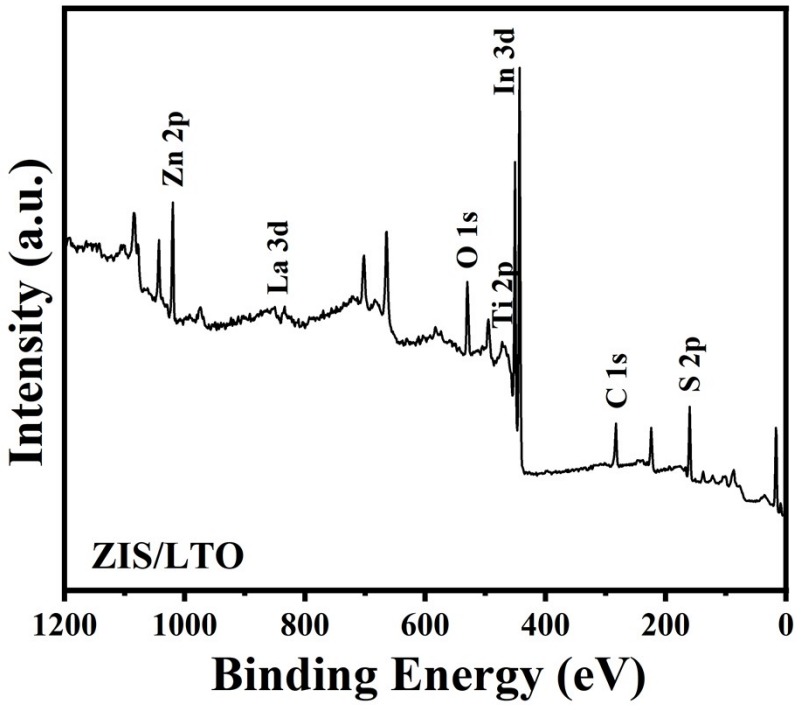

Figure S8. XPS spectra of ZIS/LTO-0.1.

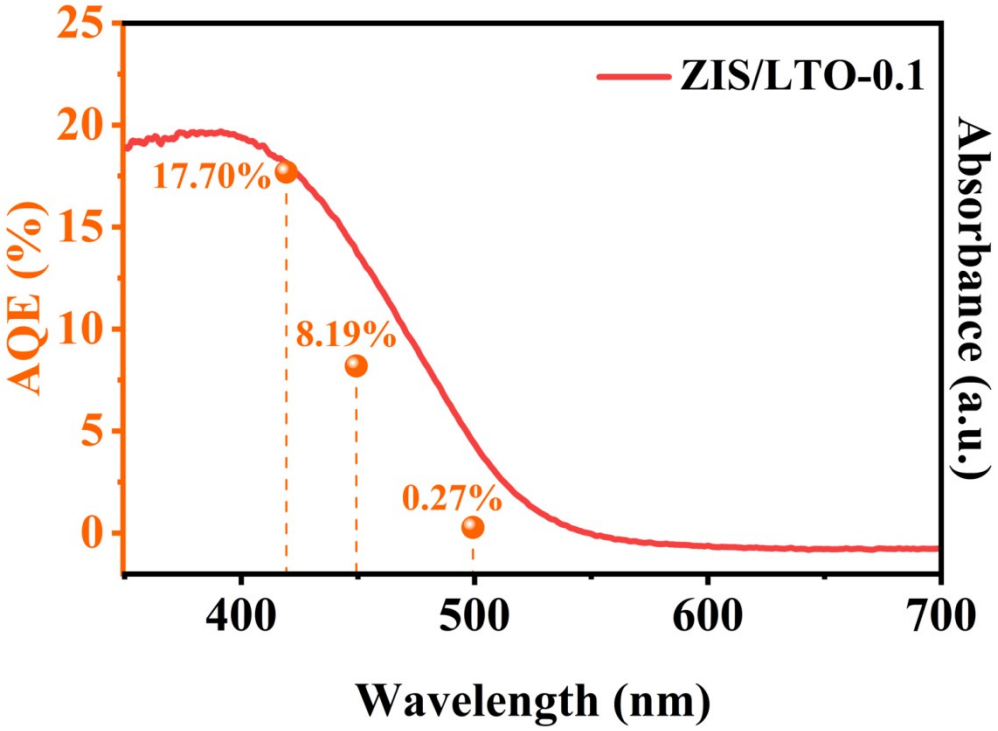

Figure S9. AQE values of ZCS@ZIS/MS at wavelengths of 420 nm, 450 nm and 500 nm.

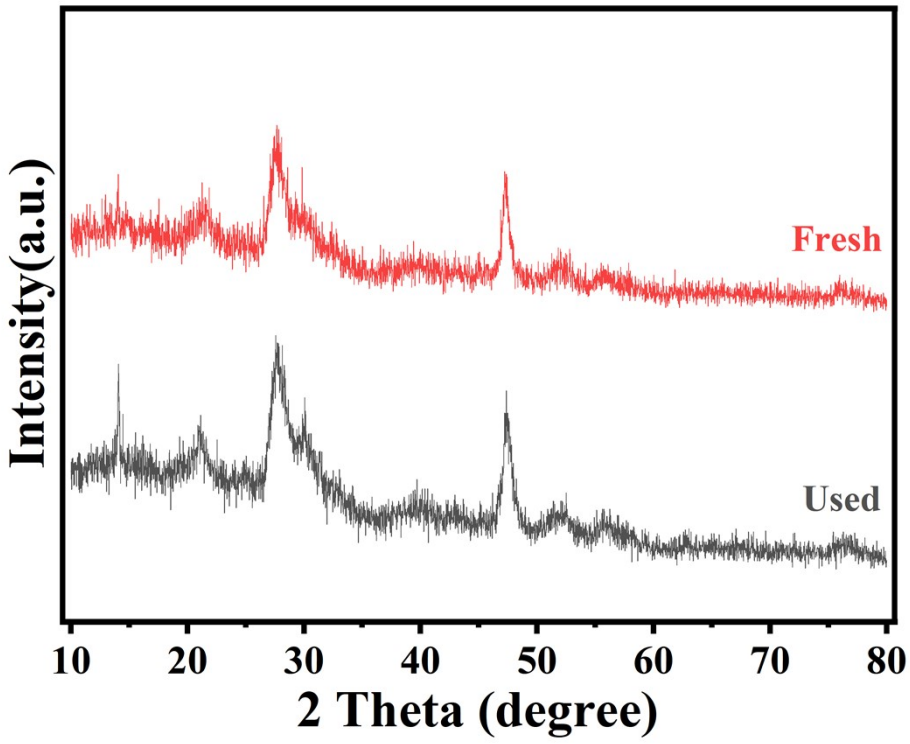

Figure S10. XRD patterns of fresh and used ZIS/LTO-0.1.

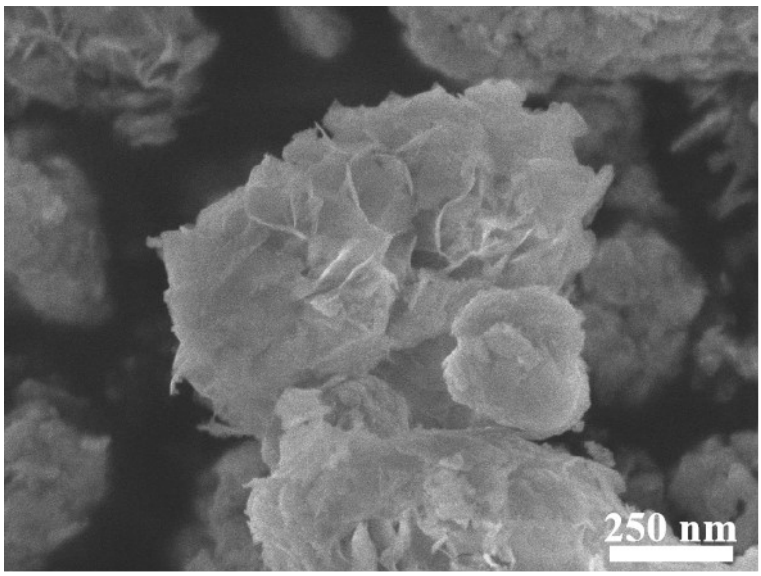

Figure S11. SEM image of ZIS/LTO-0.1 after photocatalysis.

Table S1. Comparison of photocatalytic H_2 generation performance with reported literatures.

Catalyst	Catalyst dosage (mg)	Reaction conditions	Light source	H_2 evolution rate (mmol h^{-1} g^{-1})	AQE (%)	co-catalyst	Ref.
2D/2D $ZnIn_2S_4/La_2Ti_2O_7$	20	100 mL aqueous solution (20.vol% TEOA)	300 W Xe lamp (UV-vis)	6.97	17.7 420 nm	/	This work
$Co_3O_4/La_2Ti_2O_7$	50	100 mL aqueous solution (10.vol% methanol)	300 W Xe lamp (UV-vis)	0.08	/	/	[1]

$CdS/La_2Ti_2O_7$	10	20 mL aqueous solution (0.35 M Na_2S/0.25 M Na_2SO_3)	500 $mW·cm^{-2}$ Xe lamp (UV-vis)	2.30	2.1 400 nm	/	[2]
$La_2Ti_2O_7/g\text{-}C_3N_4$	50	100 mL aqueous solution (10.vol% TEOA)	LED lamp (λ = 420nm)	1.49	3.6 420 nm	Pt	[3]
$La_2Ti_2O_7/In_2S_3$	60	100 mL aqueous solution (0.05 M Na_2S/Na_2SO_3)	300 W Xe lamp(λ ≥ 400 nm)	0.16	/	Pt	[4]
rGO/$La_2Ti_2O_7$/NiFe -LDH	20	40 mL aqueous solution (10 vol.% TEOA)	100 $mW·cm^{-2}$ Xe lamp (UV-vis-NIR)	0.53	/	/	[5]
$ZnIn_2S_4$@$In(OH)_3$ @CdS	30	100 mL aqueous solution (20 vol. % lactic acid)	300W Xe lamp (λ > 420 nm)	1.38	19.2 420 nm	/	[6]
$ZnIn_2S_4/B\text{-}C_3N_4$	20	100 mL aqueous solution (10 vol.% TEOA)	300W Xe lamp (λ ≥ 420 nm)	0.88	/	/	[7]

$ZnIn_2S_4/FePO_4$	50	100 mL aqueous solution (0.35 M Na_2S/0.25 M Na_2SO_3)	300W Xe lamp (λ ≥ 420 nm)	3.34	4.7 420 nm	/	[8]
$Co_3O_4@ZnIn_2S_4$	100	275 mL aqueous solution (20 vol.% TEOA)	300 W Xe lamp (λ > 420 nm)	4.47	20.2 420 nm	/	[9]
$ZnIn_2S_4/Cu_2MoS_4$	50	100 mL aqueous solution (0.35 M Na_2S/0.25 M Na_2SO_3)	300 W Xe lamp (λ > 420 nm)	1.30	4.7 420 nm	/	[10]
$ZnIn_2S_4/SnS_2$	50	100 mL aqueous solution (10 vol.% TEOA)	300 W Xe lamp (λ ≥ 420 nm)	1.13	9.8 420 nm	/	[11]
$Fe\text{-}Ni_2P/ZnIn_2S_4$	5	50 mL aqueous solution (15 vol.% TEOA)	300 W Xe lamp (λ > 420 nm)	4.51	29.3 420 nm	/	[12]
$Nb_2O_5/ZnIn_2S_4$	10	100 mL aqueous solution (10 vol.% TEOA)	300 W Xe lamp (λ > 400 nm)	5.40	3.3% 420 nm	/	[13]

$ZnIn_2S_4/BiFeO_3$	50	100 mL aqueous solution (0.35 M Na_2S/0.25 M Na_2SO_3)	300 W Xe lamp (λ > 420 nm)	2.88	15.7 420 nm	/	[14]
$ZnIn_2S_4/Mo_2TiC_2$	100	100 mL aqueous solution (10 vol.% TEOA)	300 W Xe lamp (λ > 420 nm)	3.12	8.6 420 nm	/	[15]

References

[1] H.D. Wen, W.N. Zhao, X.X. Han, Constructing $Co_3O_4/La_2Ti_2O_7$ p-n Heterojunction for the Enhancement of Photocatalytic Hydrogen Evolution, Nanomaterials 12(10) (2022) 12101695, http://dx.doi.org/10.3390/nano12101695.

[2] L. Mao, X.Y. Cai, M.S. Zhu, Hierarchically 1D CdS decorated on 2D perovskite-type $La_2Ti_2O_7$ nanosheet hybrids with enhanced photocatalytic performance, Rare Met. 40(5) (2021) 1067-1076, http://dx.doi.org/10.1007/s12598-020-01589-w.

[3] K. Wang, L.S. Jiang, X.Y. Wu, G.K. Zhang, Vacancy mediated Z-scheme charge transfer in a 2D/2D $La_2Ti_2O_7$/g-C_3N_4 nanojunction as a bifunctional photocatalyst for solar-to-energy conversion, J. Mater. Chem. A 8(26) (2020) 13241-13247, http://dx.doi.org/10.1039/d0ta01310b.

[4] E.B. Hua, S. Jin, X.R. Wang, S. Ni, G. Liu, X.X. Xu, Ultrathin 2D type-II p-n heterojunctions $La_2Ti_2O_7/In_2S_3$ with efficient charge separations and photocatalytic hydrogen evolution under visible light illumination, Appl. Catal. B-Environ. 245 (2019) 733-742, http://dx.doi.org/10.1016/j.apcatb.2019.01.024.

[5] R. Boppella, C.H. Choi, J. Moon, D.H. Kim, Spatial charge separation on strongly coupled 2D-hybrid of rGO/$La_2Ti_2O_7$/NiFe-LDH heterostructures for highly efficient noble metal free photocatalytic hydrogen generation, Appl. Catal. B-Environ. 239 (2018) 178-186, http://dx.doi.org/10.1016/j.apcatb.2018.07.063.

[6] L.G. Ma, C. Lin, W.J. Jiang, L. Xu, Y.J. Shao, T.Y. Zhu, T. Zhao, X.Q. Ai, X.S. Wu, In-situ constructing $ZnIn_2S_4$@$In(OH)_3$@CdS heterostructure for efficient photocatalytic H_2 generation under visible light irradiation, Int. J. Hydrogen Energy 57 (2024) 290-300, http://dx.doi.org/10.1016/j.ijhydene.2024.01.007.

[7] P.F. Tan, M.Y. Zhang, L. Yang, R.F. Ren, H.H. Zhai, H.L. Liu, J.Y. Chen, J. Pan, Modulated band structure in 2D/2D $ZnIn_2S_4$/B-C_3N_4 S-scheme heterojunction for photocatalytic hydrogen evolution, Diamond Relat. Mater. 140 (2023) 110456, http://dx.doi.org/10.1016/j.diamond.2023.110456.

[8] S.K. Wang, D. Zhang, D.F. Zhang, X.P. Pu, J.C. Liu, H.S. Li, P.Q. Cai, A novel hydrangea-like $ZnIn_2S_4/FePO_4$ S-scheme heterojunction via internal electric field for boosted photocatalytic H_2 evolution, J. Alloys Compd. 967 (2023) 171862, http://dx.doi.org/10.1016/j.jallcom.2023.171862.

[9] S.Y. Zhang, G.X. Zhang, S.Z. Wu, Z.J. Guan, Q.Y. Li, J.J. Yang, Fabrication of Co_3O_4@$ZnIn_2S_4$ for photocatalytic hydrogen evolution: Insights into the synergistic mechanism of photothermal effect and heterojunction, J. Colloid Interface Sci. 650 (2023) 1974-1982, http://dx.doi.org/10.1016/j.jcis.2023.07.147.

[10] S.K. Wang, D.F. Zhang, P. Su, X.T. Yao, J.C. Liu, X.P. Pu, H.S. Li, P.Q. Cai, In-situ preparation of mossy tile-like $ZnIn_2S_4/Cu_2MoS_4$ S-scheme heterojunction for efficient photocatalytic H_2 evolution under visible light, J. Colloid Interface Sci. 650 (2023) 825-835, http://dx.doi.org/10.1016/j.jcis.2023.07.052.

[11] C.M. Zhang, J. Ma, H.B. Zhu, H.H. Ding, H.H. Wu, K.H. Zhang, X.L. Zhao, X.F. Wang, C.L. Cheng, Self-assembled $ZnIn_2S_4/SnS_2$ QDs S-scheme heterojunction for boosted photocatalytic hydrogen evolution: Energy band engineering and mechanism, J. Alloys Compd. 960 (2023) 170932, http://dx.doi.org/10.1016/j.jallcom.2023.170932.

[12] G.Q. Li, H.O. Liang, X.Y. Fan, X.L. Lv, X.W. Sun, H.G. Wang, J. Bai, Modulating and optimizing 2D/2D Fe-$Ni_2P/ZnIn_2S_4$ with S vacancy through surface engineering for efficient photocatalytic H_2 evolution, J. Mater. Chem. A 11(27) (2023) 14809-14818, http://dx.doi.org/10.1039/d3ta02519e.

[13] H. Su, H.M. Lou, D.J. Yang, D.W. Gao, Y.X. Pang, X.Q. Qiu, 0D/2D $Nb_2O_5/ZnIn_2S_4$

heterojunctions with enhanced utilization of light and separation of photogenerated carrier for efficient visible light photocatalytic performance, Appl. Surf. Sci. 629 (2023) 157455, http://dx.doi.org/10.1016/j.apsusc.2023.157455.
[14] D.F. Zhang, R.Q. Zhang, J.C. Liu, X.P. Pu, P.Q. Cai, 3D/2D $ZnIn_2S_4/BiFeO_3$ as S-scheme heterojunction photocatalyst for boosted visible-light hydrogen evolution, J. Am. Ceram. Soc. 106(8) (2023) 4785-4793, http://dx.doi.org/10.1111/jace.19135.
[15] Q. Xi, F.X. Xie, J.X. Liu, X.C. Zhang, J.C. Wang, Y.W. Wang, Y.F. Wang, H.F. Li, Z.B. Yu, Z.J. Sun, X. Jian, X.M. Gao, J. Ren, C.M. Fan, R. Li, In Situ Formation $ZnIn_2S_4/Mo_2TiC_2$ Schottky Junction for Accelerating Photocatalytic Hydrogen Evolution Kinetics: Manipulation of Local Coordination and Electronic Structure, Small 19(24) (2023) 2300717, http://dx.doi.org/10.1002/smll.202300717.